PCCP

PAPER

View Article Online
View Journal | View Issue

Cite this: *Phys. Chem. Chem. Phys.*, 2016, **18**, 12108

Synthesis of double-wall nanoscrolls intercalated with polyfluorinated cationic surfactant into layered niobate and their magnetic alignment†

Yu Nabetani,*[ab] Akino Uchikoshi,[a] Souki Miyajima,[a] Syed Zahid Hassan,[a] Vivek Ramakrishnan,[a] Hiroshi Tachibana,[ab] Masafumi Yamato[a] and Haruo Inoue*[ab]

Received 7th March 2016,
Accepted 30th March 2016

DOI: 10.1039/c6cp01547f

www.rsc.org/pccp

The orientation of nanomaterials with an anisotropic nature such as nanoscrolls is very important for realizing their efficient and sophisticated functions in devices, including nanostructured electrodes in artificial photosynthetic cells. In this study, we successfully synthesized a nanoscroll by intercalation of a cationic polyfluorinated surfactant into the interlayer spaces of layered niobate and successfully controlled its orientation by applying an external magnetic field in water. The exfoliated niobate nanosheets were efficiently rolled-up to form nanoscrolls, which have a fine layered structure (d_{020} = 3.64 nm), by mixing with heptafluorobutanoylaminoethylhexadecyldimethylammonium bromide (C3F-S) in water, whereas the corresponding hydrocarbon analogue (C3H-S) did not form nanoscrolls. The synthetic yield for the purified and isolated nanoscrolls from the nanosheets was estimated to be 62% by weight. It was confirmed by atomic force microscopy (AFM) that most of the niobate nanosheets (98%) were converted to nanoscrolls. An external magnetic field was applied to the nanoscrolls to force them to align. After the magnetic treatment, the orientation of the nanoscrolls was investigated by small angle X-ray scattering (SAXS) and transmission electron microscopy (TEM). The non-uniform ring distribution of the SAXS patterns indicates that the nanoscrolls dispersed in water were aligned well on applying the magnetic field. The long axis of the nanoscroll was oriented in the direction of the applied field and long nanoscrolls were aligned more efficiently. When the intercalated C3F-S molecules were removed from the nanoscrolls by treating with an acid, the resultant nanoscrolls did not exhibit magnetic alignment, strongly suggesting that C3F-S plays an important role in the orientation control of the nanoscrolls by the magnetic field.

Introduction

Many types of molecular assemblies and supramolecular systems have been studied and developed extensively in the past several decades.[1] In recent years, supramolecular systems coupled with a surrounding micro-environment have attracted considerable attention for realizing much more sophisticated functions. A layered compound is one of the most attractive materials as a microenvironment, which can provide interesting interlayer spaces with a two-dimensional flat area and large flexibility in the normal direction. For example, in porphyrin/clay hybrid systems, the regulated arrangement of dye molecules[2] and the highly efficient energy transfer between the arranged molecules[3] have been achieved by matching the size of the molecule with the controlled charge density of the clay surface. Polyfluorinated compounds are also expected to be one of the most interesting materials for constructing supramolecular systems because of their unique characteristics such as hydrophobicity, lipophobicity, high solubility of gases, high resistance to oxidation and high stability against strong acids and bases. In polyfluorinated surfactant/clay hybrids, the microenvironment provides unique functions such as excess amount of molecular adsorption over cationic exchange capacity (CEC),[4] enhanced aggregation of cationic dyes,[5] inhomogeneous micropolarity[6] and gas adsorption[7] in the interlayer spaces. Furthermore, a three-dimensional reversible morphological change of hybrid film, which is based on nanosheet sliding and the shrinkage and expansion of the interlayer spaces by photo-irradiations, have been successfully found in the hybrid composed of layered niobate and polyfluorinated surfactant, including an azobenzene moiety.[8,9] A photo-responsive nanoscroll has also been successfully synthesized by the intercalation of a polyfluoroalkyl azobenzene

[a] *Department of Applied Chemistry, Graduate School of Urban Environmental Sciences, Tokyo Metropolitan University, 1-1, Minami-osawa, Hachioji, Tokyo 192-0397, Japan. E-mail: nabetani@tmu.ac.jp, inoue-haruo@tmu.ac.jp*
[b] *Center for Artificial Photosynthesis, Tokyo Metropolitan University, 1-1, Minami-osawa, Hachioji, Tokyo 192-0397, Japan*

† Electronic supplementary information (ESI) available: Fig. S1. 2D selected area electron diffraction (SAED) patterns of nanoscrolls in the TEM. See DOI: 10.1039/c6cp01547f

derivative into potassium hexaniobate, $K_4Nb_6O_{17}$, by a two-step ion exchange method.[10]

Tubular nanomaterials, such as carbon nanotubes,[11,12] which are ordinarily synthesized by arc-discharge evaporation,[12] chemical vapor deposition[13,14] and laser vaporization,[15] have also attracted considerable attention for many types of potential applications, including conducting and high-strength composites, energy conversion devices, sensors, and light-emitting devices. As a type of multi-layered nanotube, a nanoscroll prepared by rolling up an exfoliated inorganic nanosheet is also one of the most interesting tubular nanomaterials, which shows unique morphology, large specific surface area and flexibility of interlayer spaces. One of the crucial points is how can they be efficiently synthesized. Though several nanoscrolls composed of niobate,[10,16–18] titanate,[16,18] carbon[19–21] and vanadium oxide[22,23] have been developed by exfoliation of the corresponding layered compounds, the actual synthetic yield has never been discussed or revealed. In this study, we successfully synthesized niobate nanoscrolls by intercalation of polyfluorinated surfactant into layered potassium hexaniobate and analyzed their layered nanostructure. The synthetic yield of nanoscrolls by a two-step guest–guest ion exchange method was quantitatively estimated for the first time by weight measurement on the isolated nanoscrolls along with thermogravimetric analysis (TGA) and atomic force microscopy (AFM).

Another curious point is whether or not the nanoscrolls with anisotropic morphology could be oriented to exhibit preferable alignment leading to more sophisticated functions of the material. In energy conversion devices such as a nanostructured electrode in an artificial photosynthetic cell, a preferable alignment of semiconducting nanoscrolls composed of single sheets should be very attractive for obtaining more efficient electron transport within the sheet than that among many nanoparticles with many contact points and substantial resistance. The semiconducting niobate nanoscrolls would be one of the typical examples to examine in this case. Among the various types of orientation control for nanomaterials such as electric and magnetic fields, polarizing light, laser trapping, convection of fluid, and rubbing, magnetic field would be one of the most effective approaches as a non-contact external perturbation to control the orientation of tubular nanomaterials because of their large anisotropic nature. A uniformly applied magnetic field can be expected to drive the rearrangement of the nanomaterials in a wide area at one time. Previously, our group reported the orientation of the layered hybrid composed of Rhodamine B and inorganic synthetic mica (Somasif Me-100) using a rotating magnetic field.[24] The Somasif layered nanosheets were well aligned perpendicular to the rotation axis of the applied field. Herein, we report that the niobate nanoscrolls can also be aligned by an external magnetic field.

The orientation of nanoscrolls placed on a substrate in a magnetic field was analyzed by small angle X-ray scattering (SAXS) and transmission electron microscopy (TEM) and was discussed in terms of the size and the intercalated surfactant to control their orientation efficiently.

Results and discussion

Synthesis of nanoscrolls

The niobate nanoscrolls were synthesized by intercalation of the polyfluorinated surfactant, heptafluorobutanoylaminoethylhexadecyldimethylammonium bromide (C3F-S), into the interlayer of potassium hexaniobate; chemical and crystal structures are shown in Fig. 1a and c. The intercalation of C3F-S into the interlayer spaces of potassium hexaniobate was performed by a two-step guest–guest ion exchange method using methyl viologen(MV)/niobate hybrid as a precursor. Fig. 2 shows the XRD pattern change of the layered hybrids on a glass plate at each step of the intercalation. The XRD peak of MV/niobate film was shifted to a smaller angle (Fig. 2(ii)). The basal spacing corresponding to the interlayer distance of the layered hybrid (MV/niobate) (d_{020}) was measured to be 2.33 nm, which is in good agreement with the intercalation of MV only into layer I to form a periodic structure with two nanosheet layers keeping layer II unchanged,[8,9,25,26] which is hereafter termed as ''double-wall''. After mixing an aqueous solution of C3F-S with the nanosheet dispersion of MV/niobate, a further peak shift to lower angle was observed, as shown in Fig. 2(iv). This indicates that C3F-S was efficiently intercalated into interlayer I of the methyl viologen/niobate hybrid and expanded the interlayer spaces by replacing the methyl viologen with C3F-S molecules. The basal spacing, d_{020}, was enlarged to 3.64 nm. On the other hand, a similar XRD peak shift was observed (Fig. 2(iii)) for the hydrocarbon analogue, C3H-S, whose chemical structure is shown in Fig. 1b. As compared with the C3F-S/niobate, the interlayer distance of C3H-S/niobate is rather small ($d_{020,C3H\text{-}S}$ = 3.46 nm). The hydrophobic and lipophobic interactions due to the perfluoroalkyl chains may give rise to a higher dense adsorption of C3F-S in the interlayer spaces with a smaller tilt angle, resulting in the large interlayer distance of the layered hybrid. Though the XRD data indicates that the two hybrid compounds, C3F-S/niobate and C3H-S/niobate, have double-wall type layered structures, no morphological information is obtained. Both the starting niobate crystal and the precursor, MV/niobate hybrid, have stacked nanosheets morphology, as already reported.[8–10] We studied what happens when the surfactants are intercalated and the morphological structures for C3F-S/niobate and C3H-S/niobate.

Observation by a microscope provides the morphological information on the layered hybrids. Fig. 3 shows the AFM, SEM and TEM images of the C3F-S/niobate and C3H-S/niobate hybrids dispersed on a glass, silicon and carbon grid substrate.

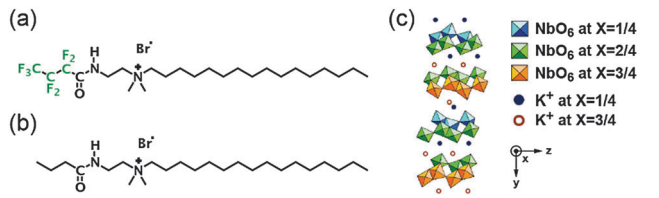

Fig. 1 Chemical and crystal structures of (a) C3F-S, (b) C3H-S and (c) potassium hexaniobate, $K_4Nb_6O_{17}$.

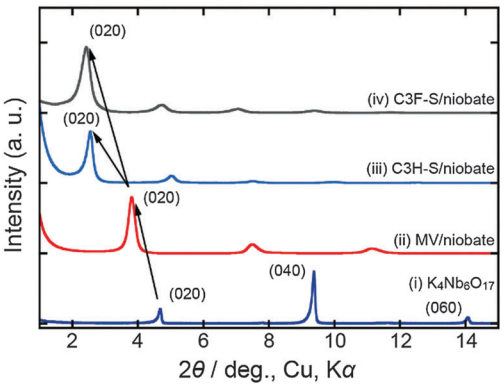

Fig. 2 XRD patterns of (i) potassium hexaniobate and the layered niobate hybrids with (ii) methyl viologen, (iii) C3H-S and (iv) C3F-S.

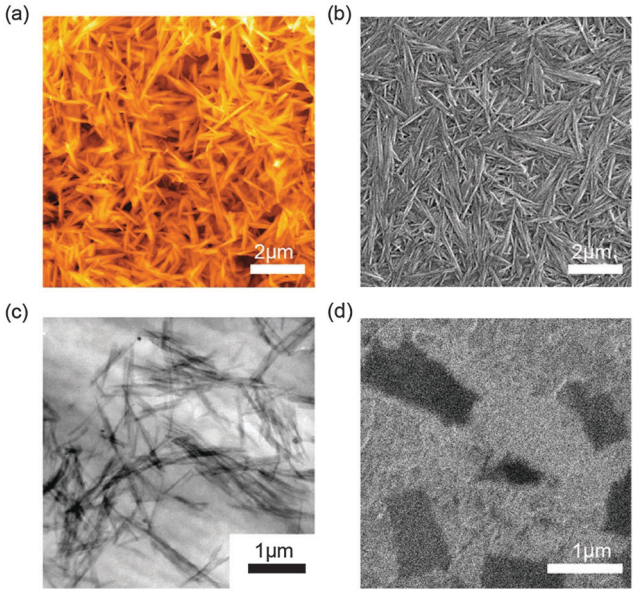

Fig. 3 Microscopic observation of the layered niobate hybrids intercalated by C3F-S and C3H-S: (a) AFM, (b) SEM and (c) TEM images of C3F-S/niobate and (d) SEM image of C3H-S/niobate.

Interestingly, many needle-like nanostructures of a few μm size on the long axis have been clearly observed only in the case of C3F-S/niobate (Fig. 3a–c). It is considered that the nanosheet as a unit of double-wall, which maintains interlayer II in the center, is rolled-up to form a scrolled structure to minimize the surface energy of the nanosheets during the stirring of the aqueous dispersion of the hybrid compounds. On the other hand, only angular dark black plates, which can be assigned to the exfoliated niobate nanosheets, were observed in the case of C3H-S/niobate, as shown in Fig. 3d. No nanoscroll could be found in C3H-S/niobate. The perfluoroalkyl group having strong hydrophobic and lipophobic properties obviously plays crucial role in the rolling-up processes.

The layered structure of the C3F-S/niobate nanoscroll was further investigated in detail by TEM and TGA. Fig. 4a and b show the side and cross-sectional TEM images for the nanoscroll of C3F-S/niobate. The layered structure was beautifully

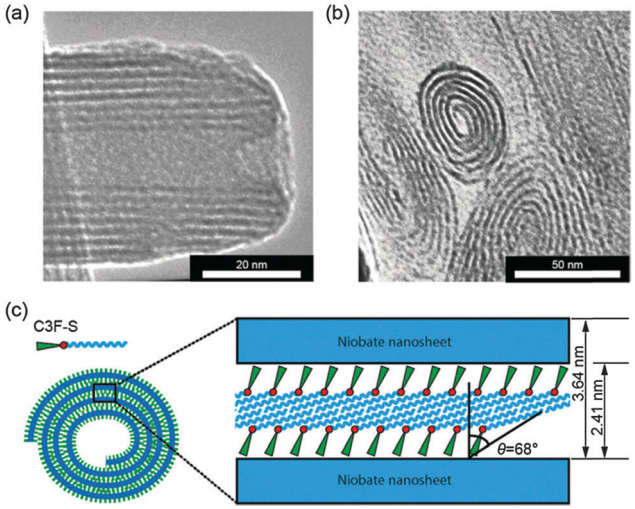

Fig. 4 Layered nanostructure of a C3F-S/niobate nanoscroll: (a) side- and (b) cross-sectional view of a nanoscroll by TEM and (c) schematic of the nanostructure of the nanoscroll: "Niobate nanosheet" represents the double-wall nanosheet keeping the layer II in the center.

observed in the TEM image of Fig. 4a as the side view of the nanoscroll. Moreover, the whorl-like pattern indicating a rolled structure of a single nanosheet was clearly observed in the cross-sectional view of Fig. 4b, though the double-wall layer looks to be a single-wall layer under the space resolution of TEM examined here. In addition to the niobate structure, the adsorbed amount of C3F-S in the interlayer space of the nanoscroll was analyzed by TGA. The C3F-S was revealed to be intercalated into the interlayer spaces and adsorbed on the surface up to 81% *versus* the CEC of the niobate nanosheet. The occupied area of adsorption by one molecule was thus estimated to be 31 $Å^2$ per molecule, which indicates that the intercalated molecules were closely packed in the interlayer spaces. If C3F-S molecules lie over the nanosheet surface without forming any aligned structures, the occupied area of adsorption should be much larger than the observed value. In the case of forming a single-layer structure, the occupied area should be also larger than 42 $Å^2$ because the two cross-sections of perfluoroalkyl (>26 $Å^2$) and long alkyl chain (>16 $Å^2$) at both the terminal ends of C3F-S should face toward the nanosheet surface. It is thus concluded that a bilayer structure of C3F-S is formed in the interlayer spaces of the niobate nanosheet as shown schematically in Fig. 4c.[4,6] The clearance space of the C3F-S/niobate hybrid was estimated to be 2.41 nm by subtraction of the nanosheet thickness (1.23 nm) from the basal spacing (3.64 nm). On the basis of the thickness of clearance space (2.41 nm) and the length of the molecule (3.18 nm) in the optimized structure of C3F-S,[27] C3F-S molecules aligned in the bilayer structure within the interlayer space can be estimated to have a tilt angle of 68°, as shown in Fig. 4c.

It is interesting to know how efficiently nanoscrolls can be synthesized by the two-step ion exchange method. Though the structural analysis of many types of nanoscroll have been reported in the past decades, very poor information was obtained on their synthetic yield, which is the most important

and fundamental parameter in material synthesis. In this study, the synthetic yields of nanoscrolls have been successfully estimated as follows. In the first step of the guest–guest ion exchange, nanosheets were exfoliated in the ion-exchanged water by the intercalation of methyl viologen into the interlayer I of niobate crystal. After the size fractionation with repeated centrifugations, a few microns of MV/niobate nanosheets were obtained with a yield of 8.4%, measured by weight. By mixing the dispersion of the exfoliated MV/niobate nanosheets with C3F-S, the nanoscroll was synthesized with a 62% yield on the basis of MV/niobate nanosheets. The overall yield of the nanoscroll from potassium hexaniobate crystal as the starting material was thus estimated to be 4.9%. In the direct morphology analysis of nanoscrolls by AFM, however, it was confirmed that 98% of the MV/niobate nanosheets (the number sampled was 407) were converted to nanoscrolls. The discrepancy may be due to substantial loss of the product during the washing processes to practically isolate the nanoscrolls to be weighed as the end products. The actual yield of nanoscrolls in the reaction system is thus considered to be almost quantitative in this case. No formation of nanoscroll in the case of the corresponding hydrocarbon analogue, C3H-S, strongly suggests that the perfluoroalkyl group in C3F-S plays crucial role in the rolling-up process through the hydrophobic and lipophobic properties, as similarly observed in the bilayer formation within clay.[4,27] The strong self-assembly property of C3F-S was also characterized in micelle and vesicle formation.[28,29]

Magnetic alignment of nanoscrolls

The orientation of nanomaterials with an anisotropic nature, such as the nanoscrolls synthesized above, is very important for potential development towards more sophisticated functions. The magnetic field, as a non-contact external perturbation, was applied to the nanoscrolls of C3F-S/niobate and their orientation was analyzed by SAXS and TEM. The schematic of the experiment for the magnetic alignment is shown in Fig. 5a. The aqueous dispersion of C3F-S/niobate nanoscrolls with an appropriate amount of polyvinyl alcohol (PVA), which can maintain the orientation of nanoscrolls, was cast over a polyvinyl carbonate substrate. During the evaporation of the solvent (water), the magnetic field was applied to the entire cast sample until the sample was dried up completely on the substrate. Among the two possible directions of alignment, parallel or perpendicular in respect to the substrate surface, the parallel alignment was adopted as the first step to examine whether or not the nanoscrolls could suffer the magnetic force, since perpendicular alignment would be more complicated due to the additional effects of gravity. The SAXS patterns were measured by irradiating X-rays onto the cast films in an axis both perpendicular to the substrate plane and the applied magnetic field direction, as shown in the right side of Fig. 5a. Fig. 5b show the SAXS patterns of the nanoscrolls cast films prepared with and without applying the magnetic fields. In Fig. 5b(i), uniform ring distribution of the SAXS pattern, which corresponds to the layered nanostructure of nanoscrolls (d_{020}), was observed for the cast film without applying a magnetic

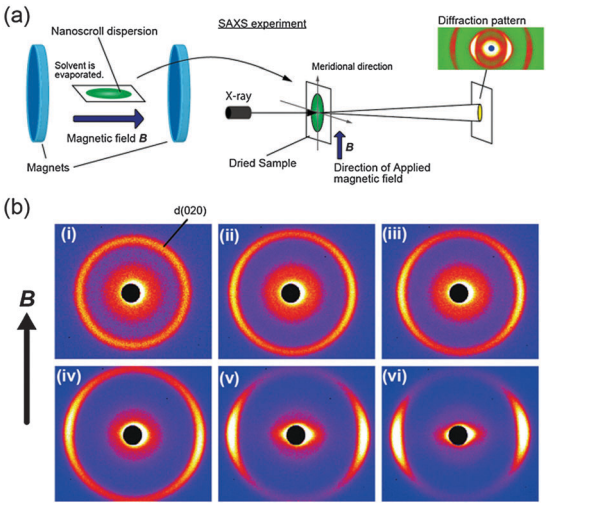

Fig. 5 (a) Schematic of the SAXS experiment and (b) the SAXS patterns of the nanoscrolls cast film prepared by applying a (i) 0, (ii) 2, (iii) 3, (iv) 5, (v) 7, and (vi) 10 T magnetic field, respectively.

field. Without a magnetic field, the nanoscrolls are homogeneously dispersed in the solution and a random orientation of nanoscrolls was left on the substrate after solvent evaporation. On the other hand, non-uniform distribution was observed for the cast film prepared by applying the magnetic field, as shown in Fig. 5b(ii)–(vi). When the magnetic field strength was increased, the strong scattering in the meridional direction was evidently observed in the SAXS pattern (Fig. 5b (ii)–(vi)). This indicates that the long axes of the nanoscrolls align in the direction of the magnetic field. The degree of orientation for the nanoscrolls was simply estimated from the SAXS patterns. Fig. 6a shows an azimuthal distribution of X-ray scattering (d_{020}) for the nanoscrolls cast film prepared with applying the magnetic field. The two peaks at around 0 and 180 degrees were clearly observed in the distribution and the degree of orientation was estimated by curve fitting with a Gaussian function. Fig. 6b shows the degree of orientation for nanoscrolls at different magnetic field strengths. With increasing magnetic field strength, the degree of orientation increased and reached 79% at 10 T. This indicates that the nanoscrolls are very efficiently aligned in the direction of the magnetic field.

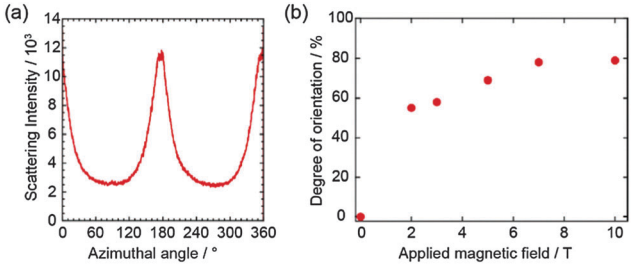

Fig. 6 (a) The azimuthal distribution of X-ray scattering (d_{020}) in the SAXS pattern for the nanoscrolls film prepared by applying a 10 T magnetic field and (b) the degree of orientation for the nanoscrolls film at different magnetic field strengths.

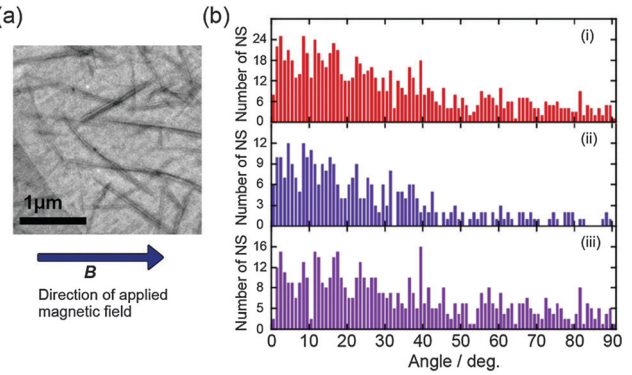

Fig. 7 (a) TEM image of nanoscroll/PVA film sliced with an ion slicer and (b) the orientation distribution of nanoscrolls by the magnetic field: (i) all the nanoscrolls, (ii) nanoscrolls longer than 800 nm and (iii) nanoscrolls shorter than 800 nm.

Previously, Eguchi *et al.* studied the anisotropic alignment of nanoscrolls by a static magnetic field.[30] In their report, the effect of the magnetic field was rather obscure and the degree of orientation could not be estimated due to the crystallographic heterogeneity of the nanoscrolls in X-ray diffraction. In our study, the evident non-uniform ring distribution in the SAXS experiment due to the nanoscrolls was successfully observed because the strong X-ray diffraction was provided by the layered fine nanostructure and sufficient amount of nanoscrolls, as shown in Fig. 3a. To directly observe the magnetic alignment of the nanoscrolls, the TEM observation was further carried out for the nanoscrolls film. Fig. 7a shows the TEM image of the nanoscrolls film prepared by applying the magnetic field (10 T), the observed area of which was cut thinly with an ion slicer.

In Fig. 7a, the nanoscrolls were partially aligned in the direction of the applied magnetic field, but not perfectly. To understand the magnetic alignment for nanoscrolls in detail, the distribution of the angle between the long axis of the nanoscroll and the direction of magnetic field was analyzed for several samples prepared in the same manner. Fig. 7b shows the angle distribution for 888 nanoscrolls in the film prepared by applying the magnetic field (10 T). A greater number of nanoscrolls was observed at around 0 degrees to the direction of the magnetic field, indicating that the nanoscrolls were surely aligned by the magnetic field. Herein, nanoscrolls longer and shorter than 800 nm were separately analyzed to investigate the size effect, which might influence their magnetic alignment. Fig. 7b(ii) and (iii) show the angle distributions for nanoscrolls longer and shorter than 800 nm, respectively. Very interestingly, the distribution for the longer nanoscrolls was more populated in the smaller angle and almost none at angles larger than 50 degrees as compared to that in Fig. 7b(iii) for the shorter nanoscrolls, which exhibit more population in the larger angles than is the case with the longer nanoscrolls. This obvious difference indicates that the longer nanoscrolls can be more effectively aligned by the magnetic field probably due to their larger magnetic dipole. Since the magnetic anisotropy of the nanoscrolls should cause magnetic alignment, the following experiment was carried out to obtain a deeper insight into which part of the hybrid, niobate nanosheet or the surfactant intercalated within the nanolayer, contributes to the anisotropy. Mallouk *et al.* discussed a possible relation between the crystal structure of potassium hexaniobate and nanoscrolls.[30,31] They claimed that the *c*-axis of the niobate crystal unit cell had a magnetic anisotropy and remained as the long axis of the nanoscroll to exhibit alignment to the direction of the magnetic field. In that case, properties of the crystal unit cell could control the scrolling-up behaviour of the nanosheet. To gain further understanding of this point, we carefully analysed whether or not any anisotropy was introduced into the nanoscroll. Very interestingly, contrary to their claim, the 2D diffraction pattern of an electron-beam of the single nanoscroll afforded no information of such anisotropy, indicating that the scrolling directions of the nanoscrolls by intercalation of C3F-S were basically random (ESI-1,†). This strongly suggests that the framework of the nanoscroll, the rolled-up niobate nanosheet, does not contribute to magnetic anisotropy. As described above, however, the long axis of the nanoscroll is actually aligned in the direction of the magnetic field. This prompted us to examine the role of surfactant within the nanoscroll. To understand the magnetic anisotropy of the nanoscroll in detail, the orientation of the nanoscrolls, from which the intercalated C3F-S molecules were partly extracted by acid, was further analysed in the same manner. Fig. 8 shows the orientation distribution of the nanoscrolls, from which 64% of C3F-S was extracted by treating with an acid. In the TEM image, it was confirmed that the layered structure of the nanoscrolls is maintained even after the partial extraction of C3F-S. Though the number of sampled nanoscrolls was rather small (106 samples), it was evident that the nanoscrolls were not aligned and rather randomly situated in the direction of the magnetic field. It is thus considered that the magnetic anisotropy of the nanoscroll might originate from the intercalated C3F-S molecules, which induce the efficient alignment of nanoscrolls.

In the previous studies on the magnetic alignment of *n*-alkane crystals[32] and peptide amphiphile,[33] it was reported that the assembled alkyl chains were aligned perpendicular to the direction of the magnetic field. The magnetic orientation could be dramatically enhanced by a cooperative assembly and

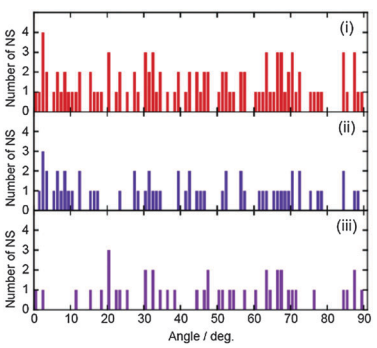

Fig. 8 The orientation distribution of nanoscrolls from which the intercalated C3F-S molecules have been partly extracted by an acid: (i) all the nanoscrolls, (ii) nanoscrolls longer than 800 nm and (iii) nanoscrolls shorter than 800 nm.

alignment of molecules, though the individual alkyl chain has a very low diamagnetic susceptibility. As revealed in this study, the intercalated C3F-S molecules are beautifully assembled in the interlayer spaces of the nanoscrolls, where the alkyl chains are aligned perpendicular to the normal direction of nanosheet albeit with a tilt angle ($\theta = 68^\circ$ in Fig. 4c). Therefore, it is considered that the long axis of a nanoscroll can be aligned in the direction of a magnetic field because the interaction in the direction normal to the nanosheet may be effectively negated due to the scrolled structure.

Experimental

Materials

Two types of cationic surfactants, heptafluorobutanoylaminoethylhexadecyldimethylammonium bromide (C3F-S) and the hydrocarbon analogue (C3H-S), were synthesized as reported elsewhere.[32,33] Their chemical structures are shown in Fig. 1a and b, respectively. Layered potassium hexaniobate ($K_4Nb_6O_{17}\cdot 3H_2O$), whose crystal structure is shown in Fig. 1c, was synthesized by heating a 2 : 3 molar mixture of Nb_2O_5 (99.95%, Kanto Chemical) and K_2CO_3 (99.95%, Kanto Chemical) at 1473 K for 20 min according to the previous procedure reported by Nassau *et al.*[34]

Synthesis of nanoscrolls

The hybrids composed of C3F-S and C3H-S with $K_4Nb_6O_{17}$ were synthesized by a two-step guest–guest ion exchange method using $(MV^{2+})_xK_{4-2x}Nb_6O_{17}$ as a precursor.[8–10] $(MV^{2+})_xK_{4-x}Nb_6O_{17}$ powder (0.1 g) was dispersed in 200 mL of ion-exchanged water and mixed with C3F-S or C3H-S aqueous solution, in which the surfactant concentration was adjusted to 3.4 mM. The molar ratio of the surfactant against MV was 19.5 : 1. Solutions were vigorously stirred at 343 K for one week. The size of the exfoliated nanosheets is adjusted to a few microns by centrifugation and washed several times with ion-exchanged water. The resulting hybrid was filtered with a PTFE membrane ($\sim$1 μm) and dried under vacuum. The interlayer distance and composition of the hybrids were characterized by X-ray diffraction (XRD, Rigaku RINT-TTR II), thermogravimetric analysis/differential thermal analysis (TGA/DTA, Shimadzu DTG-60H) and their morphology was observed by atomic force microscopy (AFM, AIST-NT) with non-contact cantilever (AIST-NT, fpN10), field emission scanning electron microscopy (FE-SEM, JEOL JSM-7500F) and high-resolution transmission electron microscopy (HRTEM, JEOL JEM-3200FS).

Magnetic alignment of nanoscrolls

Polyvinyl alcohol (PVA, MW = 2000, Kanto Chemical) was used to preserve the orientation of nanoscrolls on a substrate while being exposed to a magnetic field. 5 mg of nanoscrolls, which were dispersed in ion-exchanged water (5 mL), was mixed with 5 mL of 10 wt% aqueous PVA. The appropriate amounts of the mixture were cast onto a polyvinyl carbonate (PVC) substrate (15 mm × 20 mm) and exposed to static magnetic fields (2, 3, 5, 7 and 10 T) at 293 K until the samples were dried up by solvent evaporation at ambient temperature, as shown in Fig. 5a. For the TEM observation, the film sample was cut thinly by an ion slicer (3.0 kV of Ar-ion beam). In comparison with nanoscrolls without C3F-S, hydrochloric acid (1 M, Kanto Chemical) was used for extracting the intercalated molecules. The extracted amount of C3F-S was analyzed by TGA. All experiments were performed at room temperature.

Conclusions

In this study, we successfully synthesized double-wall nanoscrolls by intercalation of a cationic polyfluorinated surfactant (C3F-S) into the interlayer spaces of layered niobate and precisely estimated the synthetic yield for the first time. In the direct microscopic observation, most of the exfoliated nanosheets were converted to nanoscrolls by the intercalation of polyfluorinated surfactant, which should be one of the most efficient approaches for synthesizing nanoscrolls. The orientation of the nanoscrolls when applying a magnetic field has been studied by SAXS and TEM. The long axis of the nanoscrolls could be well aligned in the direction of the applied field. The driving force for the magnetic alignment of the nanoscrolls in water was concluded to be the diamagnetic susceptibility of the intercalated C3F-S molecules, which are beautifully assembled in the interlayer spaces of a nanoscroll. More efficient magnetic alignment and more sophisticated functionality of the nanomaterials could be expected through design and synthesis of the intercalated molecules.

Acknowledgements

This study was partially supported by a Grant-in-Aid for Young Scientists (B) from the Ministry of Education, Culture, Sports, Science and Technology of Japan. We would like to thank Mr Eiichi Watanabe, who is an expert in TEM experiments, for the direct observation of the nanoscrolls.

Notes and references

1 J.-M. Lehn, *Supramolecular Chemistry: Concepts and Perspectives*, VCH, Weinheim, 1995.
2 Y. Ishida, T. Shimada, H. Tachibana, H. Inoue and S. Takagi, *J. Phys. Chem. A*, 2012, **116**, 12065–12072.
3 Y. Ishida, D. Masui, H. Tachibana, H. Inoue, T. Shimada and S. Takagi, *ACS Appl. Mater. Interfaces*, 2012, **4**, 811–816.
4 T. Yui, H. Yoshida, H. Tachibana, D. A. Tryk and H. Inoue, *Langmuir*, 2002, **18**, 891–896.
5 L. A. Lucia, T. Yui, R. Sasai, S. Takagi, K. Takagi, H. Yoshida, D. G. Whitten and H. Inoue, *J. Phys. Chem. B*, 2003, **107**, 3789–3797.
6 T. Yui, S. R. Uppili, T. Shimada, D. A. Tryk, H. Yoshida and H. Inoue, *Langmuir*, 2002, **18**, 4232–4239.
7 M. Sumitani, Y. Tanamura, T. Hiratani, T. Ohmachi and H. Inoue, *J. Phys. Chem. Solids*, 2005, **66**, 1228–1233.

8 Y. Nabetani, H. Takamura, Y. Hayasaka, T. Shimada, S. Takagi, H. Tachibana, D. Masui, Z. Tong and H. Inoue, *J. Am. Chem. Soc.*, 2011, **133**, 17130–17133.
9 Y. Nabetani, H. Takamura, Y. Hayasaka, S. Sasamoto, Y. Tanamura, T. Shimada, D. Masui, S. Takagi, H. Tachibana, Z. Tong and H. Inoue, *Nanoscale*, 2013, **5**, 3182–3193.
10 Z. Tong, S. Takagi, T. Shimada, H. Tachibana and H. Inoue, *J. Am. Chem. Soc.*, 2006, **128**, 684–685.
11 S. Iijima, *Nature*, 1991, **354**, 56–58.
12 S. Iijima and T. Ichihashi, *Nature*, 1993, **363**, 603–605.
13 J. Kong, A. M. Cassell and H. Dai, *Chem. Phys. Lett.*, 1998, **292**, 567–574.
14 K. Hata, D. N. Futaba, K. Mizuno, T. Namai, M. Yumura and S. Iijima, *Science*, 2004, **306**, 1362–1364.
15 F. Kokai, K. Takahashi, M. Yudasaka, R. Yamada, T. Ichihashi and S. Iijima, *J. Phys. Chem. B*, 1999, **103**, 4346–4351.
16 R. Ma, Y. Bando and T. Sasaki, *J. Phys. Chem. B*, 2004, **108**, 2115–2119.
17 G. B. Saupe, C. C. Waraksa, H.-N. Kim, Y. J. Han, D. M. Kaschak, D. M. Skinner and T. E. Mallouk, *Chem. Mater.*, 2000, **12**, 1556–1562.
18 Y. Kobayashi, H. Hata, M. Salama and T. E. Mallouk, *Nano Lett.*, 2007, **7**, 2142–2145.
19 R. Bacon, *J. Appl. Phys.*, 1960, **31**, 283–290.
20 L. M. Viculis, J. J. Mack and R. B. Kaner, *Science*, 2003, **229**, 1361.
21 S. F. Braga, V. R. Coluci, S. B. Legoas, R. Giro, D. S. Galvao and R. H. Baughman, *Nano Lett.*, 2004, **4**, 881–884.
22 H. J. Muhr, F. Krumeich, U. P. Schönholzer, F. Bieri, M. Niederberger, L. J. Gauckler and R. Nesper, *Adv. Mater.*, 2000, **12**, 231–234.
23 F. Krumeich, H. J. Muhr, M. Niederberger, F. Bieri, B. Schnyder and R. Nesper, *J. Am. Chem. Soc.*, 1999, **121**, 8324–8331.
24 T. Kimura, T. Uemura, T. Kimura, S. Takagi and H. Inoue, *Macromol. Symp.*, 2006, **242**, 120–125.
25 T. Nakato, K. Kuroda and C. Kato, *Chem. Mater.*, 1992, **4**, 128–132.
26 T. Nakato, K. Kuroda and C. Kato, *J. Chem. Soc., Chem. Commun.*, 1989, 1144–1145.
27 T. Yui, S. Fujii, K. Matsubara, R. Sasai, H. Tachibana, H. Yoshida, K. Takagi and H. Inoue, *Langmuir*, 2013, **29**, 10705–10712.
28 Y. Kameo, S. Takahashi, M. Krieg-Kowald, T. Ohmachi, S. Takagi and H. Inoue, *J. Phys. Chem. B*, 1999, **103**, 9562–9568.
29 H. Kusaka, M. Uno, M. Krieg-Kowald, T. Ohmachi, S. Kidokoro, T. Yui, S. Takagi and H. Inoue, *Phys. Chem. Chem. Phys.*, 1999, **1**, 3135–3140.
30 M. Eguchi, M. S. Angelone, H. P. Yennawar and T. E. Mallouk, *J. Phys. Chem. C*, 2008, **112**, 11280–11285.
31 E. C. Sklute, M. Eguchi, C. N. Henderson, M. S. Angelone, H. P. Yennawar and T. E. Mallouk, *J. Am. Chem. Soc.*, 2011, **133**, 1824–1831.
32 H. H. Shao, H. Gang and E. B. Sirota, *Phys. Rev. E: Stat. Phys., Plasmas, Fluids, Relat. Interdiscip. Top.*, 1998, **57**, R6265–R6268.
33 D. W. P. M. Löwik, I. O. Shklyarevskiy, L. Ruizendaal, P. C. M. Christianen, J. C. Maan and J. C. M. van Hest, *Adv. Mater.*, 2007, **19**, 1191–1195.
34 K. Nassau, J. W. Shiever and J. L. Bernstein, *J. Electrochem. Soc.*, 1969, **116**, 348–353.

